# Boundary Layer Arc Behavior (Ii)

Author(s): R. J. Rosa

Session Name: Generators

SEAM: 22 (1984)

SEAM EDX URL: https://edx.netl.doe.gov/dataset/seam-22

EDX Paper ID: 1040

# BOUNDARY LAYER ARC BEHAVIOR (II)

R. J. Rosa

Montana State University
Bozeman, Montana 59717, U.S.A.

## ABSTRACT

The objective of this work is to understand what determines the size of the arcs on the electrodes of an MHD generator and, in particular, to predict how arc size will vary with generator size.

In an MHD generator an arc exists in a region of exceedingly steep gradients. References 1 and 2 presented an analysis of how an arc might behave under such conditions and made some preliminary comparisons with experiment. In this paper a more refined analysis and more detailed comparison with experiment are presented. Also presented is a projection of how arcs will behave in a commercial sized, coal fired generator.

## NOMENCLATURE

| | | | |
|---|---|---|---|
| $A^+$ | Nondimensional sublayer thickness = $Au_c C_{f/2}/$ | $Re_x$ | Reynolds No. |
| | | $Re_k$ | Roughness Reynolds No. |
| B | Magnetic flux density | U | Gas velocity, $U_a$, in arc column $U_c$, in core flow |
| $C_f$ | Friction coefficient | | |
| $E_a$ | Effective voltage gradient in the arc column = $E + U_a B$ | x | Arc column dimension in flow direction |
| $\Delta h$ | Arc enthalpy - ambient enthalpy | y | Distance from wall |
| $I_a$ | Arc current | y+ | Distance from wall, nondimensionalized = $yU_c C_f/2$ / |
| $\dot{j}$ | Current density$\mu$ $J_s = \sigma_c Q_o/\delta$ | z | Arc column dimension perpendicular to flow direction |
| $k_s$ | Effective roughness height | | |
| $P^+$ | Nondimensional pressure gradient = $\frac{\mu(dP/dx)}{\rho^{1/2}\tau^{3/2}}$ | $\beta$ | Hall parameter |
| | | $\rho$ | Gas density, $\rho_a$, in arc column |
| $\Delta Q$ | Increase in heat transfer | $\sigma_c$ | Electrical conductivity in core |
| $Q_o$ | Heat transfer in the absence of joule heating | $\tau$ | Shear stress: $\tau_o$, at wall |

## REFINEMENTS TO THE MODEL

In References 1 and 2 the energy balance equation for the arc column was assumed to be,

$$I_a E_a = \rho_a U_a \Delta h z \tag{1}$$

where z is the cross-sectional dimension of the column perpendicular to the direction of flow and the column was assumed to be round. A refinement introduced since then is to determine the width of the column in the x or flow direction by assuming that the arc creates a stream (or wake) of hot gas which subsequently decays by losing heat to the cooler surrounding gas stream. This leads to the following approximate formula for the x dimension,

$$x_w = \frac{\rho_a U_a C_p Z^2}{4k}$$

where $\rho_a$ and $U_a$ are the density and velocity in the arc column.

The thermal conductivity, k, is assumed to be the effective molecular plus turbulent conductivity in the boundary layer at the point in question. If the arc was a solid cylinder (like a hot wire anemometer), one might expect that only molecular conduction should be used. However, the arc is not solid, and at a typical column Reynolds number co-moving gas streams like this are unstable. Therefore, it seems reasonable that some sort of turbulent conduction or mixing process takes place and it seems reasonable that the process is influenced by the ambient turbulence. The assumption stated above follows as the most straightforward and convenient one to make. Equation 1 is still used for the energy balance, but the equation linking current, electric field and column dimensions becomes,

$$I = \sigma_a E_a Z X_w = \sigma_a E_a \rho_a C_p Z^3/(4k)$$

The rest of the derivation proceeds as outlined in references 1 and 2.

A second refinement has been to incorporate a boundary layer profile more accurate than the previous power law profile. This is important because typically in a generator the arc will be confined to a region relatively close to the wall where a power law profile is not particularly accurate. The profile is calculated using Prandtl mixing length theory and the Van Driest assumption for the sublayer (3). A pressure gradient is allowed for by assuming shear stress varies according to,

$$\tau/\tau_o = 1 + P^+ y^+ \tag{2}$$

and the effective sublayer thickness varies according to,

$$A^+ = 25/(1 + 30.2P^+) \tag{3}$$

where $y^+$, $p^+$, and $A^+$ are the typical law-of-the-wall coordinates and are defined in the list of symbols. Roughness is accounted for by adding

$$y_o = 0.031\ k_s \tag{4}$$

to the value of y appearing in the formula for the mixing length and by

reducing the sublayer thickness, A, by the factor $1/(1+R_{ek})$ where $R_{ek}$ is the roughness Reynolds number. The friction factor is assumed to be,

$$C_f/2 = .0287Re_x^{-.2} \quad \text{or} \quad C_f/2 = 0.168/(\ln(848/k_s))^2 \qquad (5)$$

whichever is larger. A laminar profile can also be selected and is necessary for interpreting some arc experiments.

The effect of joule heating on the shape of the enthalpy profile is simulated by the cubic equation proposed by Gertz et.al. (4). Values of the relative rise in heat transfer, $\Delta Q/Q_o$, are obtained from the following approximate formula:

$$\frac{\Delta Q}{Q_o} = 0.0622\ J - 0.02(1 - e^{-5J})$$

where,

$$J = (1 + \beta^2)^{1/4}\ j/J_s$$

which is my curve fit to the results of numerical integrations performed at Avco (5).

With the model described above, the effect of various profile-shaping factors such as roughness, Mach number, pressure ratio, and Reynolds number have been studied and found to have a significant effect on arc behavior. In particular, the incorporation of these effects has made it possible to correlate experimental results that previously seemed inconsistent.

One rather striking result is illustrated in Figure 1. Here the predictions of the model for two different conditions are contrasted. One set of conditions is typical of a large slag coated MHD generator channel, the other is typical of a small bench scale arc experiment. In the case of the latter, the boundary layer is laminar and it is generally found experimentally that current per arc varies quite slowly with increasing core or diffuse current density. This the model now predicts, while at the same time predicting a much steeper dependence in a generator. The difference can be understood in terms of the difference in electrical conductivity profiles. In a laminar profile on a cold wall the conductivity is negligible until close to the outer edge of the boundary layer. Consequently for all core currents, the arc length is nearly equal to the boundary layer thickness. The model links arc current to arc length and therefore if one is invariant so is the other.

On the other hand, in a turbulent boundary layer on a warm wall, conductivity increases more or less smoothly with distance from the wall. Therefore as core current density increases arc length and arc current increase also.

## COMPARISON WITH EXPERIMENT

In the following, the predictions of the model are compared with several experimental observations. The conditions are listed in Table 1 and the

results are summarized in Figures 2 through 7. In many cases, some of the input conditions are not known and had to be estimated. In all but a few cases arc current is not known since the objective has been merely to determine the onset of arcing. In order to make these experiments useful for this study it is then necessary to estimate what the current is at which an arc first becomes observable.

Very few systematic measurements of arc current vs some parameter or other are reportd in the literature. Generally observations consist of statements to the effect that, for example, an arc current of 1 to 2 amps was observed when current density was in the vicinity of 1/2 to 1 amp per square centimeter. Consequently, in the figures that follow, observations are generally not plotted as points but as cross-hatched regions of somewhat uncertain extent.

In Figure 2, the curves show predicted arc current vs core current density for the Avco Mark 6 conditions described by Petty, Demirjian, and Solbes in reference 6. Arc currents of 2 to 4 amperes were observed at a current density of about 1 Amp. per sq. cm. Theory agrees with experiment quite well if an effective roughness height of 1 mm is assumed, which is not unreasonable. A curve for a roughness height of 0.1 mm is included to show the significant difference that roughness makes. Also shown is the effect of varying boundary layer thickness up or down by a factor of two.

Figure 3 compares theory and experiment for Mark 6 and 7 conditions described by Sadovnik in Refs. 7 and 8. Again arc current is well predicted for a slagged wall. Two slag surface temperatures are given bracketing the range of reported temperatures. Voltage for slagged and unslagged conditions also seems well predicted. For the unslagged condition theory predicts a much higher arc current than the one ampere that was observed. However, it was reported that during unslagged operation, the 'arc module', a separately loaded segment of a channel electrode bar, never contained more than one arc spot at a time. This suggests that the arc current would have been higher but for the external loading of the module. This also, of course, illustrates an external way of controlling arc size.

A great deal of data on the stability of slag coated electrode walls has been collected at Stanford. From this data, a stability limit for the slag has been determined (Ref. 9, 10) and is reproduced on Figure 4 in the form of a curve of critical core current density vs. the temperature of the electrode surface underlying the slag. Now the plasma boundary layer properties are determined by the exposed slag surface temperature, which varies hardly at all with the temperature of the underlying surface (Ref. 10), hence the plasma model, on this graph, generates a series of horizontal lines as shown for an assumed slag surface temperature of 1700 K. These lines are drawn for arc currents of .03, .1, and .3 Amp. since it generally seems that it is somewhere in this range that arcs first become observable. Since these lines lie above the slag stability limit the inference is that under the conditions of this experiment the first appearance of arcs is caused by instability in the slag, not the plasma, except when interface and slag surface temperatures are about equal.

Two interesting questions now arise. The first is, will the slag control the first appearance of an arc under all conditions of interest? The second is, will the slag control the size of the arc once you are up to full

operating current? Figure 5 is an attempt to answer both of these questions. The two solid lines contrast predicted arc currents for typical Stanford and Avco Mark 6 conditions. The cross-hatched areas indicate the observed arc currents and core current densities in the two facilities. In both facilities the interface temperature was about 600 K and the slag stability limit was about .02 Amp per sq. cm. If we assume that arcs are first seen when they carry .1 Amp. then we can draw an arc current vs. Faraday core current curve for the slag as shown. The inference then is that the slag determines the first appearance, i.e. the stability limit, in both cases while the ultimate size of the arc is determined in the Stanford facility by the slag but in the Mark 6 by the plasma. In a larger generator the model would predict greater control of the arc current by the plasma, as is shown by the curve labeled '100MWE.' It seems, however, that the first appearance of arcs continues to be determined by the slag layer.

It is frequently observed that arc spots burn through the slag layer leaving a region of bare metal downstream. Perhaps this occurs when the control of arc size has transferred from the slag to the plasma.

The next series of experiments to be discussed are those performed in relatively small facilities. The first, described in Ref. 12 is small enough so that the boundary layer is laminar. No slag is present. The current density at which 'micro' arcs are first observed and at which micro arcs grow into 'mini' arcs is indicated on Figure 6. The observed anode voltage drop is also shown. The solid lines on Figure 6 are generated by the theoretical model for arc current and anode voltage under the reported experimental conditions. Agreement with experiment is fair. The voltage predicted by the model is in the right ball-park but exhibits a quite different slope. Predicted arc current is consistent with experiment if we assume that arcs are first observed when they carry 0.2 amperes. The predicted effect of wall temperatures is also consistent with experiment. Both agree that the effect of wall temperature, under these particular conditions, is very small. The experimentally observed transition to a larger arc occurs at about the j where the model predicts arc length will exceed boundary layer thickness, which seems like a reasonable reason for a discontinuity in arc behavior.

Reference 13 presents observations made in another laminar flow situation. In this case the transition to arcing is inferred from the change in slope of the voltage current characteristic. Figure 7 shows measured and calculated V-I curves. Agreement is not very good unless a boundary layer thickness twice the expected value is fed into the model. Possibly the geometry of the entrance region in this experiment generates an effectively thick boundary layer but more probably it is due to limitations of the model. Even with a thickened boundary layer the model does not well predict the voltage at a current less than .01 amp. per sq. cm.

There are at least two reasons why the present model may not work well for this experiment. First, at such a low velocity the validity of the flow-through assumption built into the arc model becomes doubtful. Second, the model entirely neglects electrostatic sheaths and other surface related effects. The first factor may account for the low voltage prediction at currents above .01 Amp. per sq. cm. and the second may account for the lack of an abrupt fall-off in voltage at currents below 0.01 Amp. per sq. cm. An effort is being made to understand and include these effects. However, it is not likely in any case that neglect of these effects seriously influences the

predictions of the model under operating conditions typical of the Mark 6 or larger generators.

Some of the most systematic experimental observations of arcs have been done in the USSR. Figure 8 compares predictions of the model with data reported by Zalkind, et al (Ref. 14) and by Zelikson et al (Ref. 15). The former describes arcs in the U0-2 on hemispherical copper electrodes, a complex situation, unfortunately, because of accelerating flow over the front of the hemisphere and the probable region of separated flow behind. To account for the acceleration, a pressure gradient of -0.05 bar/meter is assumed in the boundary layer calculation. The second set of data, that due to Zelikson et al, was obtained on a 'Temp' test stand with flat but slightly protruding electrodes.

In neither case is a complete history of the flow prior to passing over the electrodes known to the author. Consequently boundary layer thickness was adjusted so as to give reasonably good agreement with the data and then the flow length and roughness required to produce this thickness was backed out. The required length turned out to be 36 cm in the case of the U0-2 and 15 cm in the case of the 'Temp' unit. Both seem reasonably consistent with other dimensions of these two facilities which are known to the author. To this extent then, the magnitude of the predicted and measured arc currents are in agreement. It is noteworthy, in any case, that the arc current vs core current density curves are in good agreement as regards slope.

The comparisons between theory and experiment which have been presented above may perhaps best be summarized as supportive of the theory but not conclusive. Clearly, more data is needed in which more parameters are better known, more systematically varied, and more nearly like those in a full scale generator. However, it is still of interest to see what the model in its present form predicts for a full scale generator.

Figure 9 plots arc current vs core current density under conditions typical of a slag coated, coal fired channel, for several values of boundary layer thickness. The latter may exceed .1 meter in a 200 MW machine and will approach one meter in a 1000 MW machine. Therefore very large arc currents are possible. However, since in a given generator the largest boundary layer thickness is found where the current density is lowest, a trajectory through a typical generator, is expected to look like that shown on Figure 9. This seems to indicate that for a slag coated, coal fired generator, arc current will not exceed 10 amperes. This is perhaps not too bad but is high enough so that one should be concerned about the things that might make it higher or lower. An example of the former is secondary flow (Ref. 16). Examples of the latter are reduced Mach number, Hall parameter, and current density (Ref. 1).

## SUMMARY AND CONCLUSIONS

The arc-boundary layer model described at the last symposium has been refined, principally by incorporating a more sophisticated boundary layer profile which allows for variation in roughness, pressure gradient, and joule heating.

Comparison between the model and experimental data has been carried out in as much detail as the data allows. Reasonably good agreement has been

obtained. the pattern of arc behavior in small facilities is shown to differ significantly from that in large facilities.

Arc current as a function of generator size (in terms of boundary layer thickness) is predicted for typical full-scale coal fired, slag coated generator conditions. The maximum current is predicted to be about ten amperes, which is not too bad, but high enough so tht one should strive to do those things that make it lower and avoid those that do otherwise.

## ACKNOWLEDGEMENT

This paper is based upon work supported by the National Science Foundation under Grant No. CPE-8200112.

## REFERENCES

1. ROSA, R. J., 'A Survey of Boundary Layer Arcing', 21st Symposium on the Engineering Aspects of MHD, p. 4.1.1-12, 1983.

2. ROSA, R. J., 'Boundary Layer Arc Behavior', 8th International Conference on MHD Electric Power Generation, Vol. 1, p. 251-259, 1983.

3. KAYS, W. and CRAWFORD, M., 'Convective Heat and Mass Transfer', Second Edition, McGraw-Hill, 1980.

4. GERTZ, J., Opar, T., Solbes, A., and Weyl, G., 'Modeling of MHD Channel Boundary Layers Using an Integral Approach', 18th Symposium on Engineering Aspects of MHD, p. B.4.1-B.4.7, June 1979.

5. PIAN, C., Avco Everett Research Laboratory,Private Communication.

6. PETTY, DEMIRJIAN, and SOLBES, 'Electrode Phenomena in Slagging MHD Channels', 16th Symposium on the Engineering Aspects of MHD, VIII.1.1-12, 1977.

7. SADOVNIK, MARTINEZ-SANCHEZ, and SOLBES, 'Electrode Arcing Phenomena in MHD Generators', 19th Symposium on the Engineering Aspects of MHD, p. 10.1.1-.11, June 1981.

8. SADOVNIK, I., 'Electrode Arcing Phenomena in MHD Generators', Ph.D. Thesis, MIT, September, 1980.

9. NELSON and KOESTER, 'Diffuse Mode Current Transport in a Slagging MHD Generator', 7th International Conference on MHD Electric Power Generation, 711-718, June 1980.

10. KOESTER and NELSON, 'Discharge Characteristics of Slagging Metal Electrodes,' 17th Symposium on the Engineering Aspects of MHD, p. c.3.1.

11. STICKLER, D. and DeSARO, R., 'Replenishment Analysis and Technology Development', 6th International Conference on MHD Electric Power Generation, p. 31-49, 1975.

12. HARMON-WEISS, UNKEL, W., CHANG, A. Y., and SCHWOERER, J., 'Anode Phenomena in MHD Generators,' 20th Symposium on the Engineering Aspects of MHD, p. 5.2.1-5, 1982.

13. OKAZAKI, K., MURAI, Y., and TANUKU, Y., 'Mechanism of Current Constriction on the Cold Electrodes of an Open Cycle MHD Power Generator,' 8th International Conference on MHD Electric Power Generation, Vol. 1, p. 260-263, 1983.

14. ZALKIND, V. I., V. V. Kirillov, A. P. Markina, A. S. Tikhotskii, and G. L. Uspenskaya, 'Experimental Investigation of Cathode Spots on Metallic Electrodes Protruding in Plasma Flow,' Journal of Applied Mechanics and Technical, 159-164 (March-April 1974), Prikladnoi Mehaniki i Tekhnicheskoi Fiziki, 2, pp. 17-23.

15. ZELIKSON, Yu, M., V. V. Kirillov, E. P. Reshetov, and B. D. Flid, 'Laws Governing the Operation of Metallic Electrodes of a Magneto-hydrodynamic Generator,' High Temperature Journal, 181, (January-February 1970), translated from Teplofizika Vysokikh Temperatur, 8, No. 1, 193.

16. DEMETRIADES, S. T., D. A. Oliver, T. F. Swean, and C. D. Maxwell, 'On the Magnetoaerothermal Instability,' AIAA paper 81-0248, 19th Aerospace Sciences Meeting, (January 12-15, 1981).

Table 1. Experimental Parameters

| Facility | Ref. | P (Atm) | $\sigma_{core}$ mho/m | $u_{core}$ (m/s) | $T_{wall}$ °K | $T_{int}$, °K | $\beta$ | $\delta_m$ | $k_s m$ | $R_j$ |
|---|---|---|---|---|---|---|---|---|---|---|
| Avco Mk 6 & 7 | 6 | 1.0 | 8.5 | 1500 | 1800 | -- | 2 | ,024 | $10^{-3}$-$10^{-4}$ | 1 |
| | 7, 8 | 0.7 | 11 | 1200 | 700-1800 | -- | | | $10^{-3}$ | 1 |
| Stanford | 9 | 0.9 | 8 | 430 | 1700-1800 | 1000-1800 | 0-1,4 | .02 | $10^{-3}$ | 1 |
| | 10 | " | " | " | | | | " | " | 1 |
| M.I.T. | 12 | 1.0 | 4.5 | 180 | 300-950 | | 0 | .0016 | | 13 |
| Toyohashi | 13 | 1.0 | 0.4 | 40 | 700-1250 | | 0 | ,004 | | 1 |
| U-02 | 14 | 1.0 | 10 | 450 | 450-650 | | 0 | .016 | $10^{-3}$ | 1 |
| "Temp." | 15 | 1.0 | 12 | 450 | 450 | | 0 | ,008 | $10^{-3}$ | 1 |

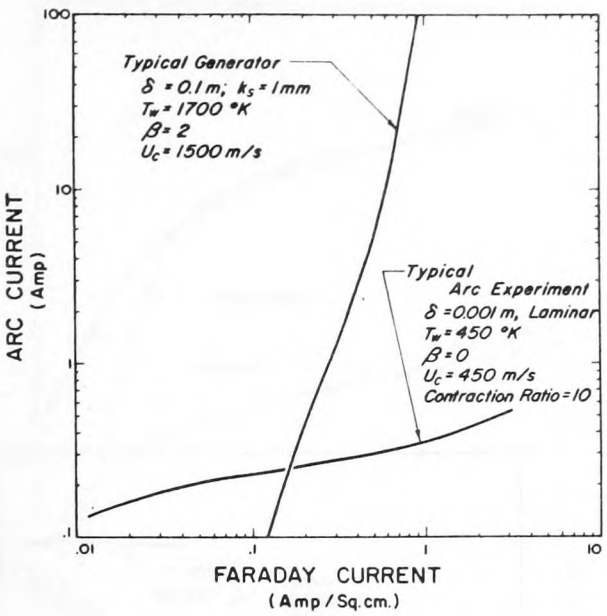


**Fig. 1. A Comparison of Arc Characteristics Typical of a Large Generator with those Typical of a Small Arc Experiment.**

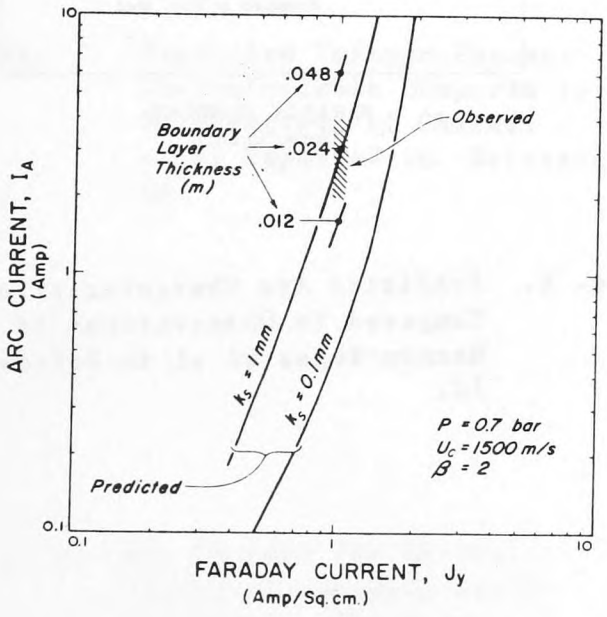


**Fig. 2. Predicted Arc Characteristics Compared to Observations in the Mark 6 Reported in Reference 6.**

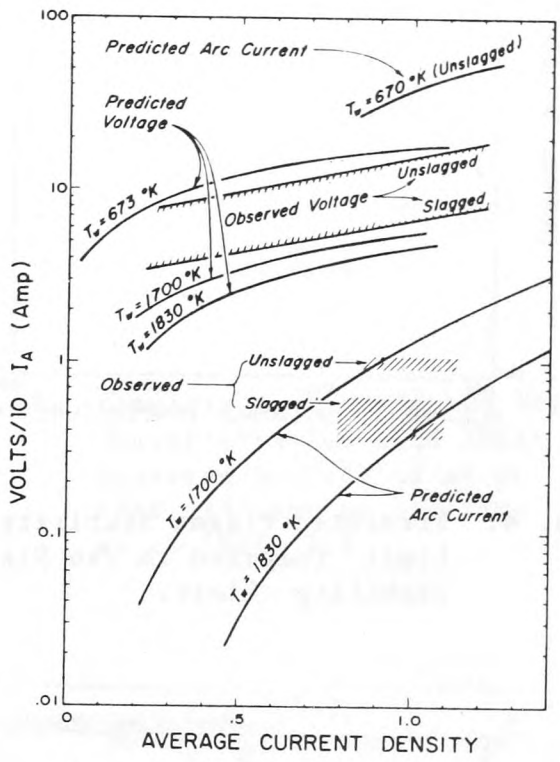


**Fig. 3. Predicted Arc Characteristics Compared to Observations in the Mark 6 Reported in References 7 and 8.**

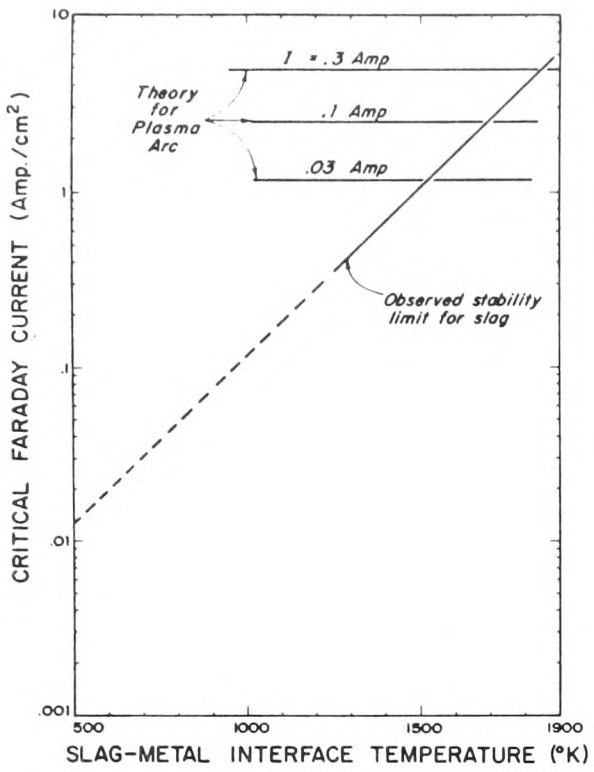


Fig. 4. Predicted Plasma Stability Limit Compared to the Slag Stability Limit.

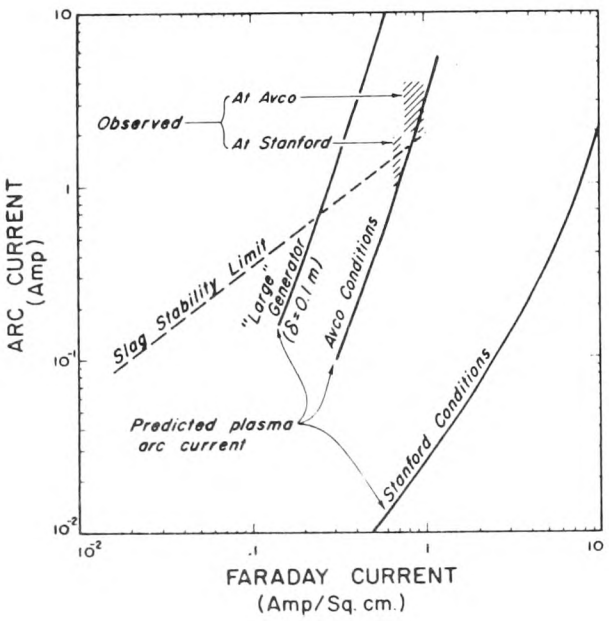


Fig. 5. Current Per Arc Spot if the Plasma Boundary Layer is in Control Compared to the Same if the Slag Layer is in Control.

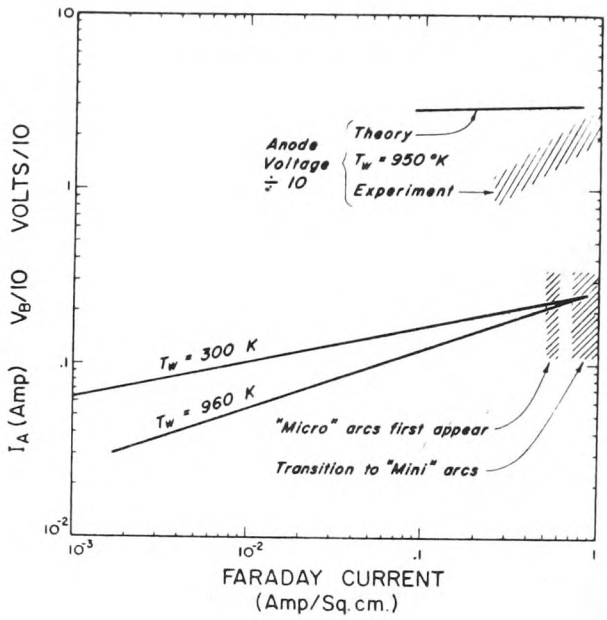


Fig. 6. Predicted Arc Characteristics Compared to Observations of Harmon-Weiss et al in Reference 12.

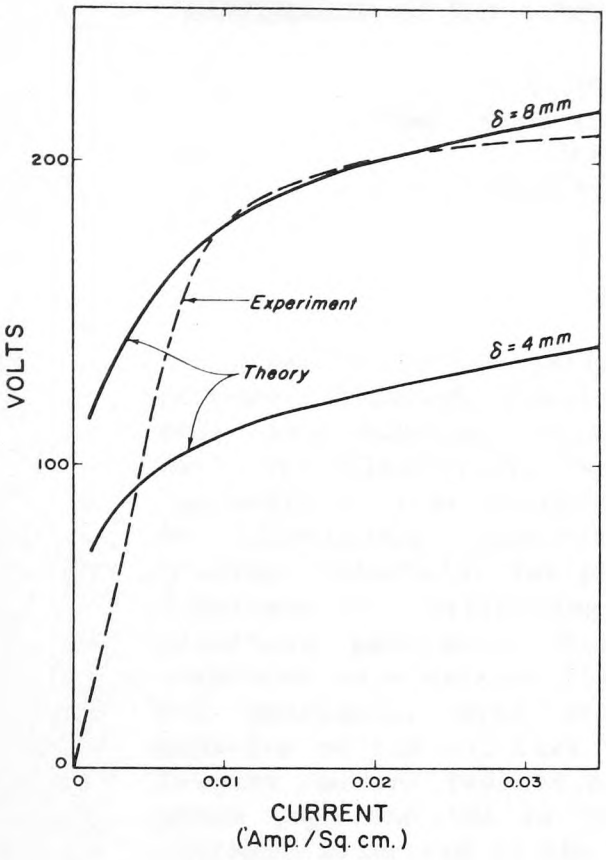


Fig. 7. Predicted Voltage-Current Characteristic Compared to Observations of Okazaki et al Reported in Reference 13.

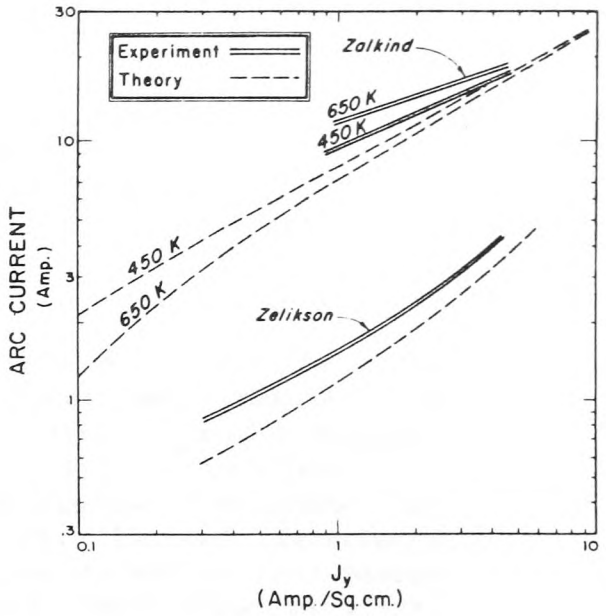


Fig. 8. Comparison of Predicted Arc Characteristics with Those Observed by Zalkind et al (Ref. 14) and by Zelikson et al (Ref. 15).

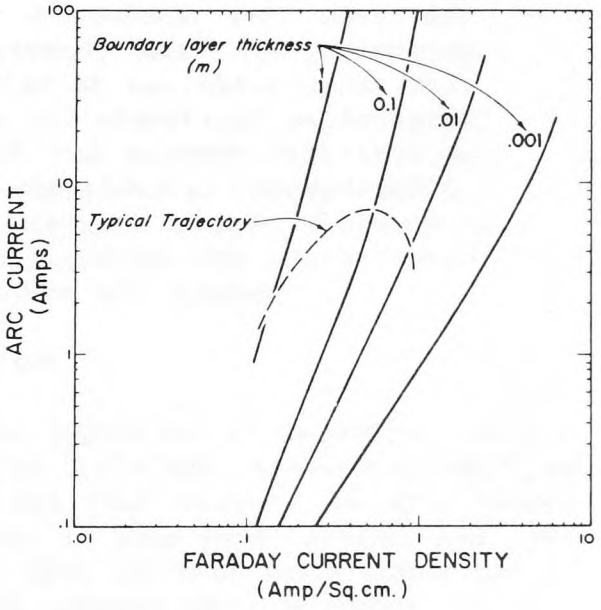


Fig. 9. Arc Current for Several Values of Boundary Layer Thickness. The curve labeled 'Typical Trajectory' traces the sequence of Faraday current-boundary layer thickness combinations encountered along the length of a typical coal-fired MHD generator design (Ref. 5).